RESEARCH BRIEF

An Oncogenic *NTRK* Fusion in a Patient with Soft-Tissue Sarcoma with Response to the Tropomyosin-Related Kinase Inhibitor LOXO-101

Robert C. Doebele[1], Lara E. Davis[2], Aria Vaishnavi[1], Anh T. Le[1], Adriana Estrada-Bernal[1], Stephen Keysar[1], Antonio Jimeno[1], Marileila Varella-Garcia[1], Dara L. Aisner[1], Yali Li[3], Philip J. Stephens[3], Deborah Morosini[3], Brian B. Tuch[4], Michele Fernandes[4], Nisha Nanda[4], and Jennifer A. Low[4]

ABSTRACT Oncogenic TRK fusions induce cancer cell proliferation and engage critical cancer-related downstream signaling pathways. These TRK fusions occur rarely, but in a diverse spectrum of tumor histologies. LOXO-101 is an orally administered inhibitor of the TRK kinase and is highly selective only for the TRK family of receptors. Preclinical models of LOXO-101 using TRK-fusion–bearing human-derived cancer cell lines demonstrate inhibition of the fusion oncoprotein and cellular proliferation *in vitro*, and tumor growth *in vivo*. The tumor of a 41-year-old woman with soft-tissue sarcoma metastatic to the lung was found to harbor an *LMNA–NTRK1* gene fusion encoding a functional LMNA–TRKA fusion oncoprotein as determined by an *in situ* proximity ligation assay. In a phase I study of LOXO-101 (ClinicalTrials.gov no. NCT02122913), this patient's tumors underwent rapid and substantial tumor regression, with an accompanying improvement in pulmonary dyspnea, oxygen saturation, and plasma tumor markers.

SIGNIFICANCE: TRK fusions have been deemed putative oncogenic drivers, but their clinical significance remained unclear. A patient with a metastatic soft-tissue sarcoma with an *LMNA–NTRK1* fusion had rapid and substantial tumor regression with a novel, highly selective TRK inhibitor, LOXO-101, providing the first clinical evidence of benefit from inhibiting TRK fusions. *Cancer Discov; 5(10); 1049–57. ©2015 AACR.*

INTRODUCTION

Tropomyosin-related kinase (TRK) is a receptor tyrosine kinase family of neurotrophin receptors that are found in multiple tissues types. Three members of the TRK proto-oncogene family have been described: TRKA, TRKB, and TRKC, coded by the *NTRK1*, *NTRK2*, and *NTRK3* genes, respectively. The TRK receptor family is involved in neuronal development, including the growth and function of neuronal synapses, memory development and maintenance, and the protection of neurons after ischemia or other types of injury (1).

TRK was originally identified from a colorectal cancer as an oncogene fusion containing 5′ sequences from the tropomyosin-3 (*TPM3*) gene and the kinase domain encoded by

[1]University of Colorado Cancer Center, Aurora, Colorado. [2]Oregon Health and Science University Knight Cancer Institute, Portland, Oregon. [3]Foundation Medicine, Cambridge, Massachusetts. [4]Loxo Oncology, South San Francisco, California.

Note: Supplementary data for this article are available at Cancer Discovery Online (http://cancerdiscovery.aacrjournals.org/).

Corresponding Author: Robert C. Doebele, University of Colorado Cancer Center, MS 8117, 12801 E. 17th Avenue, Aurora, CO 80045. Phone: 303-724-2980; Fax: 303-724-3889; E-mail: robert.doebele@ucdenver.edu

doi: 10.1158/2159-8290.CD-15-0443

the 3′ region of the neurotrophic tyrosine kinase, receptor, type 1 gene (*NTRK1*; refs. 2, 3). TRK gene fusions follow the well-established paradigm of other oncogenic fusions, such as those involving *ALK* and *ROS1* that have been shown to drive the growth of tumors and can be successfully inhibited in the clinic by targeted drugs (4, 5). Oncogenic TRK fusions induce cancer cell proliferation and engage critical cancer-related downstream signaling pathways, such as MAPK and AKT, as recently reviewed by Vaishnavi and colleagues (6). The discovery of numerous oncogenic rearrangements involving not only *NTRK1* but also the related TRK family members *NTRK2* and *NTRK3*, and the demonstration that these oncogenes can be targeted by kinase inhibitors, has renewed interest in this oncogene family (6, 7). Although there are numerous different 5′ gene fusion partners identified, all share an in-frame, intact TRK kinase domain. This high variability observed in the 5′ gene partner is similar to ROS1, where at least 25 different 5′ partners have been identified; however, all studied variants seem to respond to targeted therapy (4, 8).

LOXO-101 (the hydrogen sulfate salt of ARRY-470, shown in Supplementary Fig. S1) is a small molecule that was designed to block the ATP binding site of the TRK family of receptors, with 2 to 20 nmol/L cellular potency against the TRKA, TRKB, and TRKC kinases (7). LOXO-101 was evaluated for off-target kinase enzyme inhibition against a panel of 226 non-TRK kinases at a compound concentration of 1,000 nmol/L and ATP concentrations near the K_m for each enzyme. In the panel, LOXO-101 demonstrated greater than 50% inhibition for only one non-TRK kinase (TNK2 IC_{50}, 576 nmol/L; ref. 7). There were neither relevant hERG inhibition nor prolonged QT findings in any preclinical species tested.

A multicenter phase I dose-escalation study in patients with advanced solid tumors (ClinicalTrials.gov no. NCT02122913) was initiated in 2014 to evaluate the safety and pharmacokinetics of LOXO-101. Patients are not required to have TRK fusions or other TRK alterations. Patients are dosed once or twice daily for 28 days of continuous dosing in escalating cohorts. Patients remain on treatment until evidence of disease progression or intolerable toxicity. Preliminary pharmacokinetic and safety data from this ongoing study indicate that free plasma levels of LOXO-101 are at biologically relevant concentrations to inhibit TRK oncogenes.

This report describes the first and only patient enrolled to date on this dose-finding study with a demonstrated TRK fusion and the rapid clinical tumor regression seen with the treatment of a selective TRK inhibitor, LOXO-101.

RESULTS

TRK Fusions Are Oncogenic Drivers That Are Inhibited by LOXO-101

We and others have previously demonstrated that cancer cells harboring oncogenic TRK can be inhibited *in vitro* and *in vivo* by drugs that target the TRK kinase family (7, 9). To demonstrate activity of LOXO-101 in preclinical models harboring different variants of TRK oncogenes, we performed proliferation assays in three cell line models harboring TRK gene fusions: CUTO-3.29 is derived from a patient with lung adenocarcinoma harboring the *MPRIP–NTRK1* gene fusion; the KM12 cell line is a colorectal cancer cell line harboring the *TPM3–NTRK1* fusion (7); and the MO-91 cell line is derived from an acute myeloid leukemia patient harboring the *ETV6–NTRK3* fusion (10). Measurement of proliferation following treatment with LOXO-101 demonstrated a dose-dependent inhibition of cell proliferation in all three cell lines (Fig. 1A–C). The IC_{50} was less than 100 nmol/L for CUTO-3.29 (Fig. 1A) and less than 10 nmol/L for KM12 (Fig. 1B) and MO-91 (Fig. 1C), consistent with the known potency of this drug for the TRK kinase family. Consistent with the inhibition of cellular proliferation, we also observed inhibition of phosphorylation of the MPRIP–TRKA oncoprotein and ERK1/2 in CUTO-3.29 cells (Fig. 1D), inhibition of TPM3–TRKA, pAKT, and pERK1/2 in KM12 cells (Fig. 1E), and inhibition of the TEL–TRKC oncoprotein (encoded by *ETV6–NTRK3*), pAKT, and pERK1/2 in MO-91 cells using low doses of LOXO-101 (Fig. 1F). pAKT was not inhibited in the CUTO-3.29 cells by LOXO-101, suggesting that AKT signaling is not TRK-dependent in this tumor.

We next determined whether LOXO-101 could inhibit tumor growth *in vivo*. Athymic nude mice injected with KM12 cells were treated with LOXO-101 orally daily for 2 weeks (Fig. 1G). Dose-dependent tumor inhibition was observed, demonstrating the ability of this selective compound to inhibit tumor growth *in vivo*. Together, these and previously published results indicate that TRK fusions are constitutively activated, regulate critical downstream signaling pathways, such as MAPK and AKT, and are inhibited by a highly specific TRK inhibitor.

Initial Patient Presentation and Characterization of the Sarcoma Tumor Sample

In September 2014, a 41-year-old woman presented with a firm mass in her left groin. Initial imaging confirmed a 10-cm mass within the musculature of the anterior thigh; open biopsy revealed an undifferentiated sarcoma. Initial staging scans demonstrated multiple bilateral 4- to 13-mm pulmonary nodules consistent with metastatic disease.

The patient's diagnostic, open tumor biopsy was tested using the FoundationOneHeme panel (Foundation Medicine). This multitarget comprehensive genomic profiling (CGP) assay using DNA and RNA sequencing of hundreds of cancer-related genes demonstrated the presence of a gene fusion encoding exons 1 to 2 of the lamin A/C gene (*LMNA*) and exons 11 to 17 of the *NTRK1* gene, resulting in the *LMNA–NTRK1* fusion gene (Fig. 2A). CGP also showed the loss of the tumor suppressor *CDKN2A/B* (not shown), but no other known oncogenic mutations.

Subsequently, a break-apart FISH assay performed on the patient's tumor sample exhibited a predominantly single 3′ *NTRK1* (red fluorescence signal) pattern in 64% of tumor nuclei, consistent with a genomic alteration involving the *NTRK1* gene locus, most likely secondary to a genomic deletion between the two genes given the location and orientation of both *LMNA* and *NTRK1* on the large arm of chromosome 1 (Fig. 2B). mRNA expression of the *LMNA–NTRK1* fusion transcript from the chromosomal deletion was confirmed by RT-PCR and sequencing (Fig. 2C).

In order to assess both protein expression and functional activity of the fusion oncoprotein, we applied a proximity ligation assay (PLA) to the patient's tumor sample. PLAs are unique because they can detect functional signaling complexes

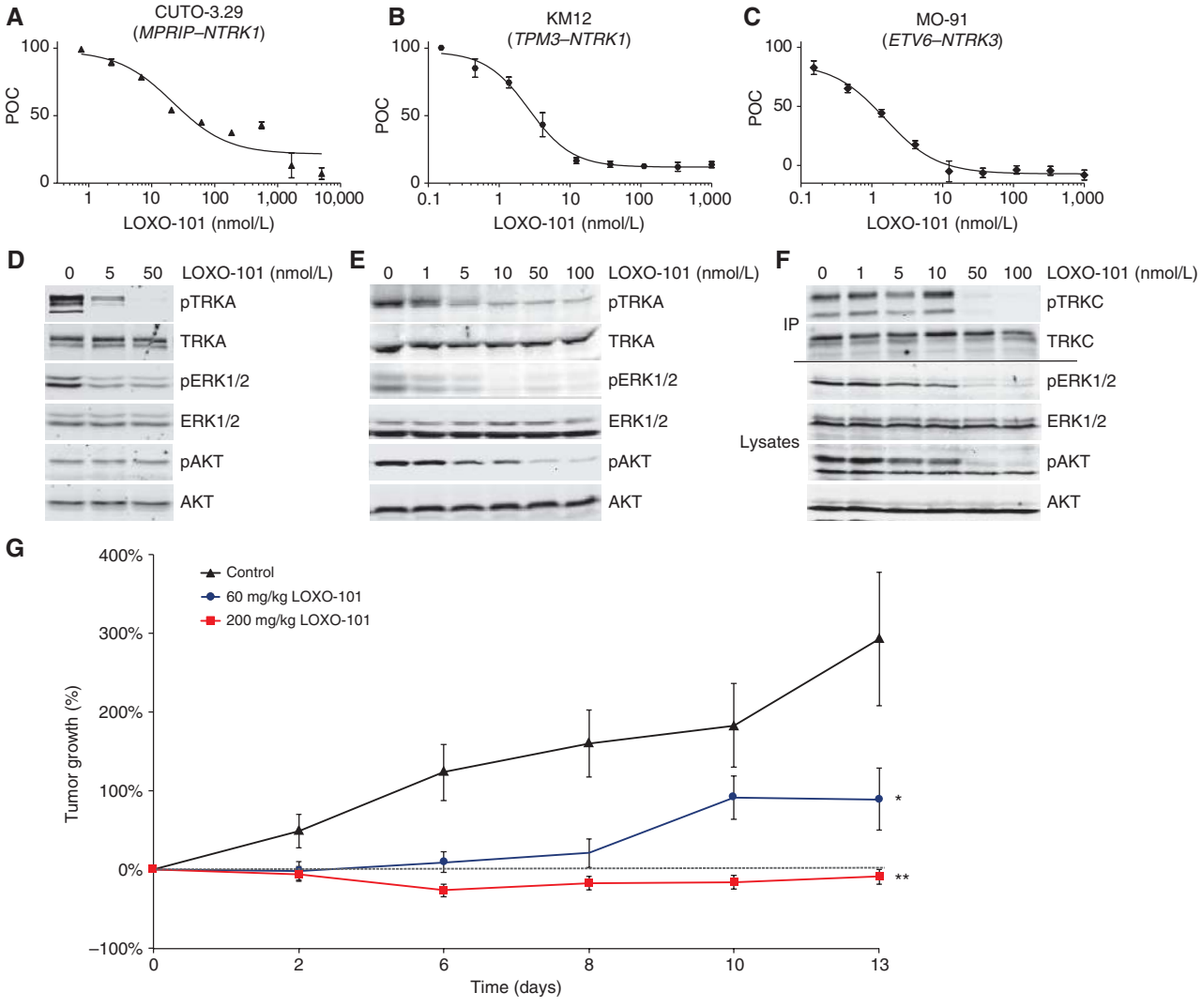

Figure 1. LOXO-101 inhibition of cancer cells harboring oncogenic TRK. **A–C,** dose-dependent inhibition with LOXO-101 is demonstrated in three cancer cell line models of oncogenic TRK. CUTO-3.29 lung adenocarcinoma with *MPRIP–NTRK1* (**A**), KM12 colorectal cancer with *TPM3–NTRK1* (**B**), and MO-91 acute myeloid leukemia with *ETV6–NTRK3* (**C**) cell lines were treated with a dose range of LOXO-101, and cellular proliferation was assayed by the MTS assay. The cellular IC_{50} was ~59.4 ± 2.2 nmol/L for CUTO-3.29; 3.5 ± 0.7 nmol/L for KM12; and 1.0 ± 0.05 nmol/L for MO-91. **D–F,** target inhibition and downstream signaling following LOXO-101 treatment in cancer cell line models of oncogenic TRK. POC, percent of control. **D,** LOXO-101 inhibits phosphorylation of Y496 of the MPRIP–TRKA kinase and phosphorylation of T202/Y204 of ERK1/2 in CUTO-3.29 cells. **E,** LOXO-101 inhibits phosphorylation of Y496 of TPM3–TRKA kinase and downstream phosphorylation of ERK1/2 and S473 AKT in KM12 cells. **F,** LOXO-101 inhibits phosphorylation of TEL-TRKC kinase and ERK1/2 and AKT phosphorylation in MO-91 cells. Cells were treated for 2 hours with the indicated doses of LOXO-101 or DMSO alone, and cell lysates were analyzed using the indicated antibodies except for MO-91 cells, which were treated for 2 hours with 100 nmol/L of LOXO-101 or DMSO alone, and cell lysates were immunoprecipitated with an anti-TRK antibody followed by immunoblot analysis with the indicated antibodies. **G,** LOXO-101 inhibits tumor growth in a KM12 colorectal xenograft model. Percent changes from baseline tumor volume in nude mice ($n = 10$/group) injected subcutaneously with KM12 cells and treated with diluent (control), 60 mg/kg/dose, or 200 mg/kg/dose daily for 14 days are shown. *P* values for comparisons between the indicated treatment group and the control group are indicated as *, $P < 0.05$ and **, $P < 0.01$.

between a kinase and one of its adaptors *in situ* (11). In this assay, we measured TRKA complexed with its preferred adaptor, SHC1, which binds to Y496 in the TRKA kinase domain (Supplementary Fig. S2; ref. 12). We have validated this assay in both human cell lines and formalin-fixed patient-derived tumor xenograft (PDX) tumor samples (Supplementary Fig. S3). RNAi knockdown of *NTRK1* disrupts TRKA–SHC1 complexes in the CUTO-3 cell line harboring the *MPRIP–NTRK1* fusion gene (Supplementary Fig. S3A–S3C), as does inhibition with the pan-TRK selective inhibitor LOXO-101 (Supplementary Fig. S3D and S3E). The TRK PLA detects functional signaling complexes in a formalin-fixed, paraffin-embedded (FFPE) tumor sample from a PDX, CULC001, harboring the *MPRIP–NTRK1* gene fusion but not the PDX CULC002, which does not harbor a known oncogenic driver mutation (Supplementary Fig. S3F and S3G). The TRK–SHC PLA can also detect non-oncogenic signaling complexes as shown by a positive signal in a region of peripheral

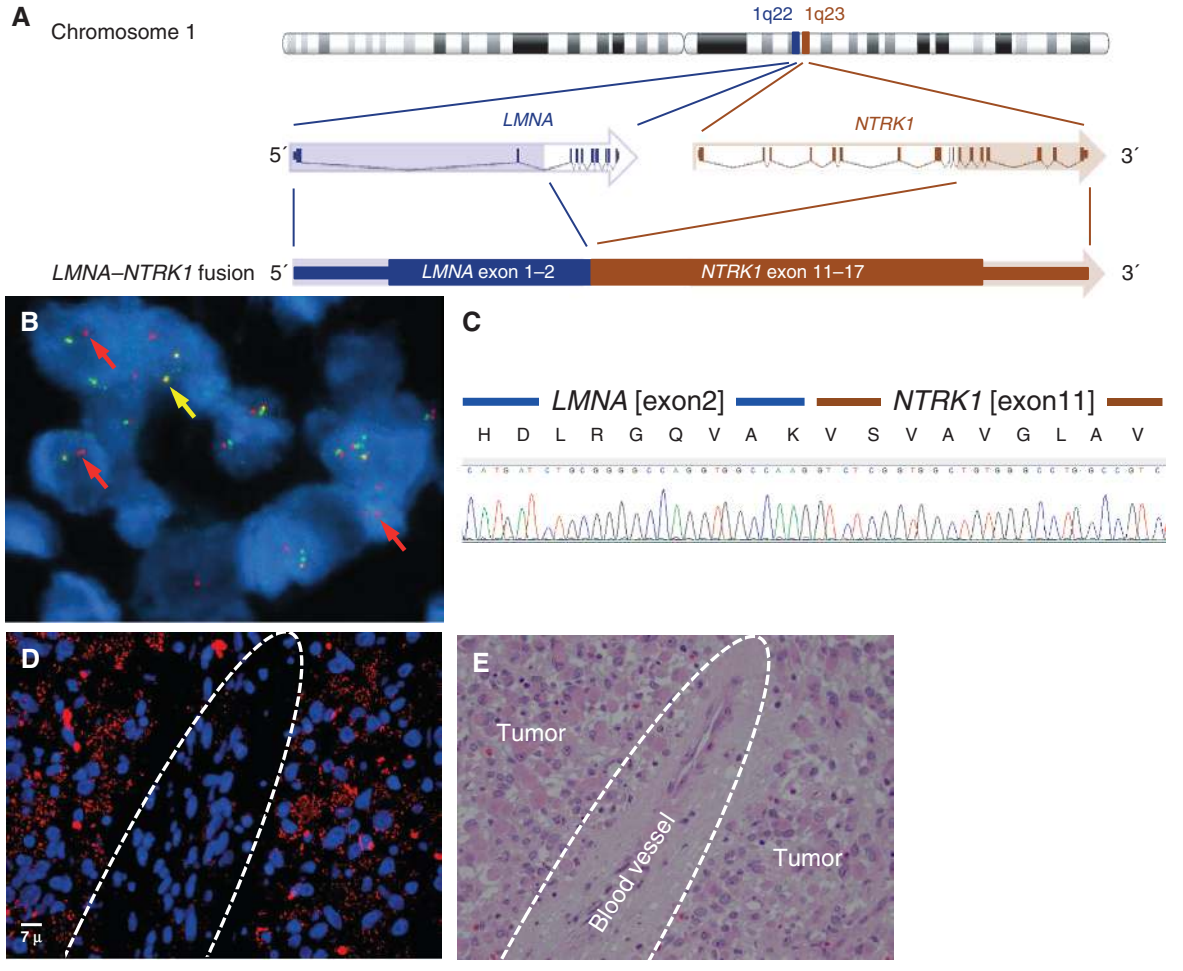

Figure 2. Molecular characterization of tumor sample. Multimodality testing demonstrating genomic, transcriptional, and functional (protein) evidence of *LMNA–NTRK1* gene fusion in the patient's tumor sample. **A,** the *LMNA–NTRK1* gene fusion was identified in the patient's tumor sample by the FoundationOneHeme panel, joining the first two exons of *LMNA* (NM_170707) with exons 11 to 17 of *NTRK1* (NM_002529). **B,** *NTRK1* break-apart FISH was performed as previously described (7) and demonstrated both paired green (5′ *NTRK1*) and red (3′ *NTRK1*) signals corresponding to the normal *NTRK1* gene (yellow arrow). Isolated red signals (red arrows) are observed in tumor nuclei (stained blue with DAPI), indicative of a chromosomal deletion leading to an *NTRK1* gene fusion. **C,** chromatograph of DNA sequencing of RT-PCR product using *LMNA* (5′) and *NTRK1* (3′) primers indicating the fusion breakpoint between exon 2 of *LMNA* and exon 11 of *NTRK1*. **D,** TRK–SHC1 proximity ligation assay demonstrates robust signaling in the tumor cells but weak signaling in the thick-walled blood vessel. Nuclei are stained with DAPI (blue), and the red signals represent a positive PLA indicative of TRKA–SHC1 protein complexes. A blood vessel is indicated within the partial ellipse (dotted white line). **E,** adjacent tumor tissue section stained with hematoxylin and eosin, indicating a thick-walled blood vessel (within partial ellipse indicated by dotted white line) and flanking tumor nuclei.

nerve tissue of the CULC001 PDX, where the TRK family of receptors have high expression and activity mediated by the neurotrophins (Supplementary Fig. S3H and S3I; ref. 13). Application of this assay to the patient's tumor sample demonstrated robust signaling associated with tumor nuclei, but only a weak signal in the blood vessel (human endothelial cells express TRKA; ref. 14) consistent with oncogenic signaling by the LMNA–TRKA oncoprotein (Fig. 2D and E). The TRK–SHC1 PLA demonstrated a negative result on a tumor sample from an ALK$^+$ non–small cell lung cancer patient, whereas the ALK–GRB2 PLA was positive (Supplementary Fig. S4A and S4B), further demonstrating the ability of this assay to detect oncogenic signaling in human tumor samples.

The presence of the *LMNA–NTRK1* fusion detected by a FoundationOneHeme assay and then validated by FISH and RT-PCR combined with the evidence of TRKA protein expression and functional activity of the TRK pathway in the patient's tumor sample suggested that the patient has a TRK-driven cancer suitable for treatment with a TRK-specific inhibitor.

The *LMNA–NTRK1* Fusion Sarcoma Patient Responds to Treatment with LOXO-101

After the initial diagnosis in September 2014, an aggressive treatment plan was agreed upon, and she enrolled on a phase II trial of sorafenib with chemotherapy, preoperative radiation, and limb-sparing surgery (ClinicalTrials.gov no. NCT02050919). After 2 weeks of sorafenib 400 mg daily, she received epirubicin 30 mg/m^2 daily and ifosfamide 2,500 mg/m^2 daily with mesna for 3 consecutive days, with continuation of daily sorafenib. The tumor became progressively more

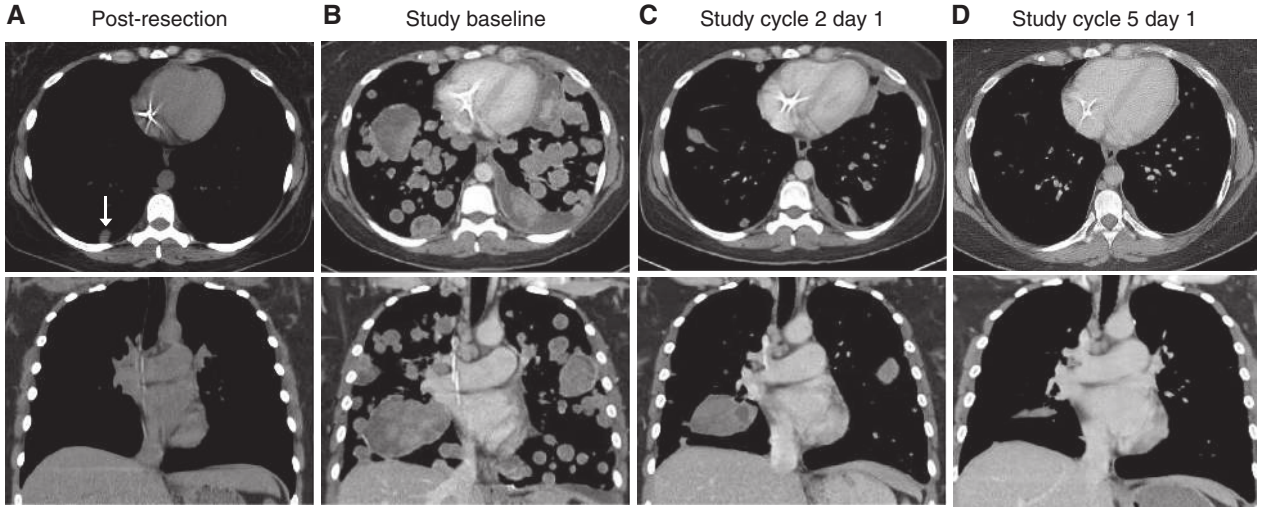

Figure 3. Radiologic response to LOXO-101. CT obtained following preoperative chemotherapy and primary tumor resection, with arrow indicating the presence of an 18-mm right lung nodule 4 months prior to starting LOXO-101 (**A**), baseline imaging just prior to dosing with LOXO-101 on study (**B**), and following 1 cycle (28 days; **C**), and 4 cycles (4 months; **D**) of dosing with LOXO-101. The patient was observed to have metastatic disease only in the lungs, and therefore the CT scan images show axial (top) and coronal (bottom) images focusing on the thoracic cavity. The images demonstrate an initial rapid disease progression (**A** and **B,** 13-week interval) followed by a marked tumor response with decreased size and/or resolution of the numerous pulmonary metastases (**B–D,** 4-week and 16-week intervals since baseline).

painful during these 5 weeks of systemic therapy. During simulation for preoperative radiation, extension of the tumor was noted cranially within the psoas muscle, precluding the safe administration of effective radiation doses due to predicted bowel toxicity. She therefore came off protocol and proceeded to surgical resection. Resection of the primary tumor achieved negative margins, and review of the pathologic specimen confirmed 90% tumor necrosis. A restaging chest CT (shown in Fig. 3A) obtained 9 weeks after initial scans showed worsening metastatic disease, with the largest nodule now measuring 18 mm. The patient's postoperative course was complicated by a polymicrobial wound infection, requiring repeated wound debridement and prolonged antibiotic therapy. Repeat chest CT was obtained before resumption of chemotherapy and demonstrated dramatic progression over the prior 9 weeks, with multiple pulmonary nodules greater than 3 cm, the largest nearly 7 cm, and a large left pleural effusion. In February 2015, after placement of a tunneled pleural drain and initiation of supplemental home oxygen, the patient received one dose of doxorubicin 75 mg/m^2 while awaiting enrollment on the LOXO-101 clinical trial.

Based on multiple lines of genetic and functional biomarker data suggesting the presence of a TRK driver oncogene, the patient was referred for consideration of enrollment into the phase I trial of LOXO-101 (ClinicalTrials.gov no. NCT02122913) in February 2015. In March 2015, the patient was found eligible for the trial and provided written informed consent. The baseline CT scan showed continued tumor progression with multiple large pulmonary metastases in both lungs, although the pleural effusion had resolved following placement of the pleural drain (Fig. 3B). On clinical presentation, the patient had significant exertional dyspnea and required 5 L of supplemental oxygen to maintain an oxygen saturation of 90%. Baseline laboratory values were notable for an elevated CA125 tumor marker level (Supplementary Fig. S5). The patient was assigned to receive LOXO-101 100 mg twice daily. During cycle 1, the patient was seen weekly for pharmacokinetic and safety data collection. No drug-related adverse events were noted, and the patient experienced weekly improvement in her exertional dyspnea during this 4-week period. The CA125 levels normalized over cycle 1. A CT was performed prior to the start of cycle 2 day 1, which demonstrated a marked improvement in multiple pulmonary metastases and was deemed a partial response by RECIST 1.1 (Fig. 3C). Additional CT scans on cycle 5 day 1 (after 4 months of LOXO-101 dosing) demonstrated almost complete tumor disappearance of the largest tumors (Fig. 3D). Clinically, the patient had significantly improved exertional dyspnea and was no longer requiring supplemental oxygen, with an oxygen saturation of 97% on room air. After 4 months of dosing, the patient did not have any adverse events that were attributed to LOXO-101.

DISCUSSION

TRK fusions have been identified as a rare subset of a number of diverse tumor histologies (15, 16). The genomic structures of these TRK fusions and the inferred protein structures have suggested that these genes are oncogenic drivers, and previously reported preclinical work in addition to that shown here supports this hypothesis (6, 7, 9). The first patient with a documented *NTRK* fusion in this clinical trial demonstrated substantial tumor regression when treated with a selective inhibitor of TRK, providing clinical validation of this molecular target.

TRK fusions are relatively unknown in soft-tissue sarcoma (STS), and this clinical response also indicates the potential for actionable molecular targets for this disease.

Table 1. Clinical characteristics of patients with STS harboring *NTRK* fusion genes

5′ Gene	5′ Last exon	3′ Gene	3′ First exon	*CDKN2A/B* deletion? (Y/N)	Disease[a]	Gender	Age
LMNA	2	*NTRK1*	11	Y	STS (nos; *n* = 179)	F	41
LMNA	10	*NTRK1*	11	Y	STS (nos; *n* = 179)	M	22
LMNA	10	*NTRK1*	12	Y	Soft-tissue fibrosarcoma (*n* = 28)	M	Under 5
SQSTM1	2	*NTRK1*	10	N	Soft-tissue fibrosarcoma (*n* = 28)	F	Under 5
TPM3	7	*NTRK1*	10	N	Soft-tissue schwannoma (*n* = 3)	M	Under 5
ETV6	5	*NTRK3*	15	N	Soft-tissue hemangioma (*n* = 4)	F	Under 5
TFG	6	*NTRK3*	14	Y	Soft-tissue solitary fibrous tumor (*n* = 28)	M	17
NTRK3	17	*HOMER2*	2	N	STS (nos; *n* = 179)	F	68

[a]*n* represents the total number of patients within each disease ontology.
Abbreviation: nos, not otherwise specified.

There is a large unmet clinical need for better treatments in advanced STS, a heterogeneous group of tumors of mesenchymal origin encompassing more than 50 histologic subtypes. More than 12,000 Americans will be diagnosed with STS this year, and 4,700 people will die from the disease (17). Inoperable metastatic STS is treated palliatively, with a median overall survival of approximately 1 year and a 5-year survival rate of less than 20% (18). The standard of care for most advanced STS subtypes remains single-agent doxorubicin, with an expected response rate of approximately 20% (19–23). Although a significant proportion of sarcomas have known chromosomal translocations that are valuable for diagnostic purposes, these alterations have generally not informed treatment decisions and have often proven to be difficult therapeutic targets. The majority of sarcoma-associated translocations involve genes encoding transcription factors, such as the pathognomonic *EWS–FLI1* fusion of Ewing sarcoma. Fusions involving kinases or growth factors have been identified in several sarcoma subtypes characterized by low metastatic potential, including dermatofibrosarcoma protuberans (DFSP). DFSP is driven by a *COL1A1–PDGFB* fusion in fibroblasts, resulting in unregulated production of mature PDGFB. Treatment with imatinib results in dramatic tumor shrinkage (24). Similarly, inflammatory myofibroblastic tumors (IMT) harbor fusions involving *ALK* or *ROS1*, and treatment with crizotinib results in rapid clinical response (25–27). The only previously known defining TRK fusion in sarcoma is the *ETV6–NTRK3* fusion in infantile fibrosarcoma, a locally aggressive but rarely metastasizing mesenchymal tumor exclusively affecting children under the age of one.

The *LMNA–NTRK1* gene fusion has been previously reported in Spitzoid nevi and is constitutively activated when expressed in cells resulting in activation of ERK1/2, AKT, and PLCγ, demonstrating its oncogenicity (9). *LMNA* has also been identified as a gene fusion partner of *ALK* (26). Foundation Medicine has previously tested 1,272 STS samples with the FoundationOne Heme CGP Test, resulting in the detection of 8 *NTRK1* or *NTRK3* fusions, including the patient described in this case report (Table 1). Thus, Foundation Medicine's detection rate for *NTRK* fusions in STS is 0.63% [95% confidence interval (CI), 0.32%–1.24%], which we believe represents a lower estimate of the true prevalence of these genetic lesions due to the complexities of sarcoma disease ontology classification and the likelihood of false negatives. Notably, 6 of the 8 sarcoma patients with *NTRK* fusions are under the age of 25 (Fisher exact test, P value = 4×10^{-4}), and 4 of the 8 are under the age of 5 (Fisher exact test, P value = 2×10^{-5}), indicating an increased detection rate of *NTRK* fusions among pediatric patients (4.1%; 95% CI, 1.8%–9.3%) and particularly those under the age of 5 (14.3%; 95% CI, 5.7%–31.5%). Also of interest, one of the gene fusions detected combines the majority of the *NTRK3* gene (exons 1–17) to the 3′ end of the *HOMER2* gene (exons 2–9), which contains a dimerization domain (coiled-coil domain), and therefore represents a 3′ gene fusion event that has been described for multiple other RTK-encoding genes, such as *EGFR*, *AXL*, and *FGFR3* (17, 28, 29). Because this patient also had a *CDKN2A/B* deletion, we decided to examine whether co-occurrence of these two lesions was common in sarcomas. We found that 4 of the 8 sarcoma patients with an *NTRK* fusion also harbored a *CDKN2A/B* deletion (Table 1); 14% of all sarcomas tested by Foundation Medicine have been found to harbor *CDKN2A/B* deletions (30).

LOXO-101 (ARRY-470) has previously been demonstrated to have no effect on cell lines that lack a TRK oncogene (7). In this report, three different cell line models, each with different tumor histologies and TRK fusions, demonstrated dose-dependent inhibition by LOXO-101 *in vitro*. Although there were subtle differences in signaling, such as AKT dependence on TRK signaling, it remains unclear whether these differences are caused by the cell context (histologic origin or genetic context) or the gene fusion itself. For example, the persistence of AKT signaling in the CUTO-3.29 cells may account for the slightly higher IC_{50} of this cell line compared with KM12 and MO-91 cells where pAKT was reduced with LOXO-101. Identification of additional patients and cell line models may help answer this question in

the future. Finally, murine xenograft experiments with a colorectal cancer cell line harboring an *NTRK1* fusion demonstrated dose-dependent inhibition of tumor growth by LOXO-101.

The tumor regression and clinical response seen in this *LMNA–NTRK1* fusion patient provide clinical validation of a new molecular target in oncology, and establish that at least this *NTRK1* fusion is a molecular driver of this patient's clinical disease. Additional follow-up of this patient to understand the durability of the response and the potential future mechanisms of resistance will be important to investigate how TRK inhibition has affected this tumor. Additional patients with this and other TRK fusions will need to be treated with this or other TRK inhibitors to understand the clinical utility of TRK inhibition in this population and other potential TRK fusion populations. Preclinical data using diverse cancer cell lines originating from different tumor types suggest that the oncogene driver may be the dominant factor in determining response to targeted therapy, rather than the histologic subtype. Molecular evaluation of all tumor types is increasingly essential to properly identify investigational and approved drugs to better treat molecularly defined cancers.

METHODS

Clinical Trial

NCT02122913 is an ongoing multicenter phase I dose-escalation study evaluating the safety and pharmacokinetics of LOXO-101, a selective pan-TRK, in unselected patients with metastatic or advanced solid tumors without standard therapy options. The study is approved by Institutional Review Boards (IRB) at all institutions that enroll patients, and eligible patients provide written informed consent to participate. The study is sponsored by Loxo Oncology and is conducted in accordance with the Declaration of Helsinki and Good Clinical Practices. LOXO-101 is a 3-urea-substituted pyrazolo[1,5a]-pyrimidine (7) provided in 100 mg capsules by the clinical trial sponsor (Loxo Oncology). CAS registry numbers for LOXO-101 include 1223403-58-4 and 1223405-08-0. Enrolled patients receive escalating doses of LOXO-101 according to a modified 3+3 design, and receive LOXO-101 daily or twice daily until intolerable toxicity, disease progression, or withdrawal of consent. In patients with measurable disease, efficacy is assessed per RECIST 1.1 criteria.

Next-Generation Sequencing

DNA and RNA were extracted and adaptor-ligated sequencing libraries were captured by solution hybridization using custom bait-sets targeting 405 cancer-related genes and 31 frequently rearranged genes by DNA-seq, and 265 frequently rearranged genes by RNA-seq (FoundationOneHeme; Foundation Medicine). All captured libraries were sequenced to high depth (Illumina HiSeq) in a Clinical Laboratory Improvements Amendment (CLIA)–certified College of American Pathologists (CAP)–accredited laboratory (Foundation Medicine), averaging >500× for DNA and >6M unique pairs for RNA. Sequence data from gDNA and cDNA were mapped to the reference human genome (hg19) and analyzed through a computational analysis pipeline to call genomic alterations present in the sample, including substitutions, short insertions and deletions, rearrangements, and copy-number variants.

FISH

NTRK1 break-apart FISH was performed on 4-μm slides from FFPE tumor samples as previously described using the Vysis LSI NTRK1 (Cen) SpectrumGreen and Vysis LSI NTRK1 (Tel) SpectrumRed (Abbott Molecular; # 08N43-030 and 08N43-020, respectively; ref. 7).

RT-PCR and DNA Sequencing

RT-PCR was performed as previously described using the forward primer to *LMNA* (LMNA F1, 5′gagggcgagctgcatgat3′; ref. 9) and the reverse primer to *NTRK1* (NTRK1 R1, 5′cggcgcttgatgtggtgaac3′). DNA sequencing of the RT-PCR product was performed using Sanger DNA Sequencing at the Pathology Core at the University of Colorado.

Cell Lines

CUTO-3 cell lines were initiated from the malignant pleural effusion of a patient with stage IV lung adenocarcinoma harboring the *MPRIP–NTRK1* gene fusion as previously described (7, 31); IRB-approved informed consent to derive immortal cell lines was obtained from the patient. CUTO-3.29 was derived from the same malignant pleural effusion by single-cell cloning. KM12 and MO-91 have been previously described (7, 10). All cell lines in this study were authenticated by DNA fingerprinting by short tandem repeat analysis using the AmpFLSTR Identifiler PCR Amplification Kit (Cat. # 4322288 from Invitrogen Life Technologies/Applied Biosystems) in July 2015 by the Barbara Davis Center Molecular Biology Service Center at the University of Colorado.

PDX Generation

IRB-approved informed consent to generate patient-derived murine xenografts was obtained from the relevant patients. Animal care and procedures were approved by the Institutional Animal Care and Use Committee Office of the University of Colorado Anschutz Medical Campus. Pleural fluid (CULC001) from a lung adenocarcinoma patient harboring an *MRPIP–NTRK1* gene fusion was centrifuged, and the resulting cell pellet was suspended in 5 mL ACK buffer (Lonza) for 2 minutes allowing for the complete lysis of red blood cells. Lysis was halted by the addition of 20 mL PBS and centrifuging the samples. The pellet was washed twice with PBS prior to being suspended in DMEM-supplemented media as above. One hundred microliters of cells (1×10^6 per flank) suspended in a 1:1 mix of DMEM and Matrigel (BD) were injected subcutaneously into the flanks of 5 nude mice. Tumor tissue from an oncogene-negative lung adenocarcinoma patient (CULC002) was cut into $3 \times 3 \times 3$ mm pieces that were transferred to DMEM supplemented with 10% FBS, 200 units/mL penicillin, and 200 μg/mL streptomycin. Tumor pieces were dipped in Matrigel (Corning) and inserted into incisions on each flank of 5 nude mice. Propagation and maintenance of resulting xenografts were previously described (32).

Proximity Ligation Assays

Cells were seeded onto glass coverslips (in a 48-well plate) or chamber slides at 25k to 75k cells/well. Cells were treated with the indicated doses and times then fixed for 15 minutes by shaking at room temperature in 4% paraformaldehyde. Cells were rinsed twice in PBS, and then the Duolink *in situ* PLA Kit from SigmaAldrich in mouse/rabbit (Red) was used according to the manufacturer's protocol (cat. # DUO92101). Antibody concentrations were optimized using immunofluorescence prior to PLA experiments. FFPE tissue PLAs from mice or patients were prepared as described in histology. In addition, samples were treated with 300 mmol/L glycine for 15 minutes prior to the blocking step; otherwise, the assay was performed according to the manufacturer's protocol. Cells were mounted using Prolong gold anti-fade reagent (with DAPI) and cured overnight prior to imaging. Images were taken either on a Nikon standard inverted fluorescent microscope at 40×, or on the 3I Marianas spinning disc confocal in the University of Colorado Anschutz Medical Campus Advanced Light Microscopy Core at 40× or 100×. The following antibodies were used: TRK (C17F1; 1:100) and ALK (D5F3; 1:200–1:400) from Cell Signaling Technology, SHC1 (1:50) from Novus, and GRB2 (610111; 1:200–1:400) from BD.

Proliferation Assays

All proliferation assays were performed in media supplemented with 5% FBS as previously described, using Cell Titer 96 MTS (Promega). Cells were seeded 500 to 2,000 cells per well and treated for 72 hours at the drug concentrations described on each graph. Each assay was performed in triplicate in at least 3 independent biologic replicates. Data were plotted, and IC_{50} values were calculated using GraphPad software.

Mouse Xenograft Studies

Athymic nude mice were obtained from Harlan Laboratories and maintained under aseptic conditions. The care and treatment of experimental animals were in accordance with institutional guidelines. KM12 cells (5×10^5) were injected subcutaneously into the dorsal flank area of the mice. Tumor volume was monitored by direct measurement with calipers and calculated by the formula: length × (width^2)/2. Following the establishment of tumor and when the tumor size was between 150 and 200 mm^2, mice were randomly selected to receive diluent, 60 mg/kg/dose, or 200 mg/kg/dose of LOXO-101. LOXO-101 was administered by oral gavage once daily for 14 days. After the last dose, tissue and blood were collected at 3, 6, and 24 hours after treatment.

Immunoblotting

Immunoblotting was performed as previously described (7). Briefly, cells were lysed in RIPA buffer with Halt Protease and Phosphatase Inhibitor Cocktail (Thermo Scientific) and diluted in loading buffer (LI-COR Biosciences). Membranes were scanned and analyzed using the Odyssey Imaging System and software (LI-COR). The following antibodies were used from Cell Signaling: pTRK Y490 (rabbit polyclonal, #9141; 1:1,000), pERK1/2 XP T202/Y204 (#9101; 1:2,000), ERK1/2 (1:2,000), pAKT S473 (rabbit mAb, #4060; 1:2,000), and AKT mouse clone D3A7 (#2920; 1:2,000). TRK (C-14) rabbit polyclonal antibody (1:1,000) was purchased from Santa Cruz Biotechnology. GAPDH (MAB374; 1:5,000) and pTYR (4G10; 1:2,000) were from Millipore.

Statistical Analysis

CIs for the detection rate of *NTRK* fusions in samples from patients with sarcoma were calculated using the 1-sample proportions test. The disease histology classification was based on the Foundation Medicine disease ontology as of April 2015. The enrichment of *NTRK* fusions in younger patient groups was tested using the Fisher exact test. All statistical testing was performed in R v 3.1.3. Comparison of treatment arms for the *in vivo* mouse xenograft studies was performed using repeated measures ANOVA with Bonferroni correction using GraphPad software.

Disclosure of Potential Conflicts of Interest

R.C. Doebele reports receiving commercial research grants from Abbott Molecular, Loxo Oncology, and Mirati Therapeutics; is a consultant/advisory board member for Loxo Oncology; and has received licensing fees from Abbott Molecular (licensed patent), Blueprint Medicines (licensed cell line), and Chugai (licensed cell line). A.T. Le has received licensing fees from Abbott Molecular (licensed patent). M. Varella-Garcia reports receiving a commercial research grant from Abbott Molecular and has ownership interest in a patent for use of FISH probes for molecular diagnosis. D.L. Aisner has received speakers bureau honoraria from AstraZeneca and Clovis. Y. Li has ownership interest in Foundation Medicine. P.J. Stephens has ownership interest in Foundation Medicine. D. Morosini has ownership interest in Foundation Medicine. J.A. Low has ownership interest in Loxo Oncology. No potential conflicts of interest were disclosed by the other authors.

Authors' Contributions

Conception and design: R.C. Doebele, L.E. Davis, J.A. Low
Development of methodology: R.C. Doebele, A. Vaishnavi, A. Estrada-Bernal, A. Jimeno, M. Varella-Garcia, B.B. Tuch, N. Nanda, J.A. Low
Acquisition of data (provided animals, acquired and managed patients, provided facilities, etc.): R.C. Doebele, A.T. Le, A. Estrada-Bernal, S. Keysar, A. Jimeno, M. Varella-Garcia, D.L. Aisner, D. Morosini, M. Fernandes, J.A. Low
Analysis and interpretation of data (e.g., statistical analysis, biostatistics, computational analysis): R.C. Doebele, A. Vaishnavi, A.T. Le, A. Estrada-Bernal, M. Varella-Garcia, Y. Li, P.J. Stephens, B.B. Tuch, N. Nanda, J.A. Low
Writing, review, and/or revision of the manuscript: R.C. Doebele, L.E. Davis, A. Vaishnavi, A.T. Le, A. Estrada-Bernal, S. Keysar, A. Jimeno, M. Varella-Garcia, D.L. Aisner, Y. Li, P.J. Stephens, D. Morosini, B.B. Tuch, M. Fernandes, N. Nanda, J.A. Low
Administrative, technical, or material support (i.e., reporting or organizing data, constructing databases): L.E. Davis, A.T. Le, B.B. Tuch, M. Fernandes, N. Nanda, J.A. Low
Study supervision: R.C. Doebele, M. Fernandes, J.A. Low

Acknowledgments

The authors thank the patient and her family for her participation in this clinical trial, and prior patients at the University of Colorado for graciously donating the tumor tissue that was used to generate cell lines and PDXs. They also thank Nikki Ayodeji and the remainder of the clinical trial staff at the University of Colorado, and Carol Hill at Loxo Oncology.

Grant Support

This study was funded by the State of Colorado and University of Colorado Technology Transfer Office Bioscience Discovery Evaluation Grant Program, the University of Colorado Lung Cancer SPORE (funded by NCI grant P50CA058187), a Loxo Oncology research grant, and a V Foundation Scholar Award (to R.C. Doebele). The study was also supported by NIH/NCI CCSG P30CA046934 (Molecular Pathology Shared Resource; to M. Varella-Garcia and D.L. Aisner).

The costs of publication of this article were defrayed in part by the payment of page charges. This article must therefore be hereby marked *advertisement* in accordance with 18 U.S.C. Section 1734 solely to indicate this fact.

Received April 15, 2015; revised July 24, 2015; accepted July 24, 2015; published OnlineFirst July 27, 2015.

REFERENCES

1. Nakagawara A. Trk receptor tyrosine kinases: a bridge between cancer and neural development. Cancer Lett 2001;169:107–14.
2. Pulciani S, Santos E, Lauver AV, Long LK, Aaronson SA, Barbacid M. Oncogenes in solid human tumours. Nature 1982;300:539–42.
3. Martin-Zanca D, Hughes SH, Barbacid M. A human oncogene formed by the fusion of truncated tropomyosin and protein tyrosine kinase sequences. Nature 1986;319:743–8.
4. Shaw AT, Ou SH, Bang YJ, Camidge DR, Solomon BJ, Salgia R, et al. Crizotinib in ROS1-rearranged non-small-cell lung cancer. N Engl J Med 2014;371:1963–71.
5. Shaw AT, Kim DW, Mehra R, Tan DS, Felip E, Chow LQ, et al. Ceritinib in ALK-rearranged non-small-cell lung cancer. N Engl J Med 2014;370:1189–97.
6. Vaishnavi A, Le AT, Doebele RC. TRKing down an old oncogene in a new era of targeted therapy. Cancer Discov 2015;5:25–34.

7. Vaishnavi A, Capelletti M, Le AT, Kako S, Butaney M, Ercan D, et al. Oncogenic and drug-sensitive NTRK1 rearrangements in lung cancer. Nat Med 2013;19:1469–72.
8. Davies KD, Doebele RC. Molecular pathways: ROS1 fusion proteins in cancer. Clin Cancer Res 2013;19:4040–5.
9. Wiesner T, He J, Yelensky R, Esteve-Puig R, Botton T, Yeh I, et al. Kinase fusions are frequent in Spitz tumors and spitzoid melanomas. Nat Commun 2014;5:3116.
10. Taipale M, Krykbaeva I, Whitesell L, Santagata S, Zhang J, Liu Q, et al. Chaperones as thermodynamic sensors of drug-target interactions reveal kinase inhibitor specificities in living cells. Nat Biotech 2013;31:630–7.
11. Smith MA, Hall R, Fisher K, Haake SM, Khalil F, Schabath MB, et al. Annotation of human cancers with EGFR signaling-associated protein complexes using proximity ligation assays. Sci Signal 2015;8:ra4.
12. Stephens RM, Loeb DM, Copeland TD, Pawson T, Greene LA, Kaplan DR. Trk receptors use redundant signal transduction pathways involving SHC and PLC-gamma 1 to mediate NGF responses. Neuron 1994;12:691–705.
13. Kaplan DR, Martin-Zanca D, Parada LF. Tyrosine phosphorylation and tyrosine kinase activity of the trk proto-oncogene product induced by NGF. Nature 1991;350:158–60.
14. Dolle JP, Rezvan A, Allen FD, Lazarovici P, Lelkes PI. Nerve growth factor-induced migration of endothelial cells. J Pharmacol Exp Ther 2005;315:1220–7.
15. Klijn C, Durinck S, Stawiski EW, Haverty PM, Jiang Z, Liu H, et al. A comprehensive transcriptional portrait of human cancer cell lines. Nat Biotechnol 2015;33:306–12.
16. Stransky N, Cerami E, Schalm S, Kim JL, Lengauer C. The landscape of kinase fusions in cancer. Nat Commun 2014;5:4846.
17. Frattini V, Trifonov V, Chan JM, Castano A, Lia M, Abate F, et al. The integrated landscape of driver genomic alterations in glioblastoma. Nat Genet 2013;45:1141–9.
18. Clark MA, Fisher C, Judson I, Thomas JM. Soft-tissue sarcomas in adults. N Engl J Med 2005;353:701–11.
19. Linch M, Miah AB, Thway K, Judson IR, Benson C. Systemic treatment of soft-tissue sarcoma-gold standard and novel therapies. Nat Rev Clin Oncol 2014;11:187–202.
20. Lorigan P, Verweij J, Papai Z, Rodenhuis S, Le Cesne A, Leahy MG, et al. Phase III trial of two investigational schedules of ifosfamide compared with standard-dose doxorubicin in advanced or metastatic soft tissue sarcoma: a European Organisation for Research and Treatment of Cancer Soft Tissue and Bone Sarcoma Group Study. J Clin Oncol 2007;25:3144–50.
21. Santoro A, Tursz T, Mouridsen H, Verweij J, Steward W, Somers R, et al. Doxorubicin versus CYVADIC versus doxorubicin plus ifosfamide in first-line treatment of advanced soft tissue sarcomas: a randomized study of the European Organization for Research and Treatment of Cancer Soft Tissue and Bone Sarcoma Group. J Clin Oncol 1995;13:1537–45.
22. Sleijfer S, Ouali M, van Glabbeke M, Krarup-Hansen A, Rodenhuis S, Le Cesne A, et al. Prognostic and predictive factors for outcome to first-line ifosfamide-containing chemotherapy for adult patients with advanced soft tissue sarcomas: an exploratory, retrospective analysis on large series from the European Organization for Research and Treatment of Cancer-Soft Tissue and Bone Sarcoma Group (EORTC-STBSG). Eur J Cancer 2010;46:72–83.
23. Sleijfer S, Seynaeve C, Verweij J. Using single-agent therapy in adult patients with advanced soft tissue sarcoma can still be considered standard care. Oncologist 2005;10:833–41.
24. Rutkowski P, Debiec-Rychter M, Nowecki Z, Michej W, Symonides M, Ptaszynski K, et al. Treatment of advanced dermatofibrosarcoma protuberans with imatinib mesylate with or without surgical resection. J Eur Acad Dermatol Venereol 2011;25:264–70.
25. Rafee S, Elamin YY, Joyce E, Toner M, Flavin R, McDermott R, et al. Neoadjuvant crizotinib in advanced inflammatory myofibroblastic tumour with ALK gene rearrangement. Tumori 2015;101:e35–9.
26. Lovly CM, Gupta A, Lipson D, Otto G, Brennan T, Chung CT, et al. Inflammatory myofibroblastic tumors harbor multiple potentially actionable kinase fusions. Cancer Discov 2014;4:889–95.
27. Butrynski JE, D'Adamo DR, Hornick JL, Dal Cin P, Antonescu CR, Jhanwar SC, et al. Crizotinib in ALK-rearranged inflammatory myofibroblastic tumor. N Engl J Med 2010;363:1727–33.
28. Seo JS, Ju YS, Lee WC, Shin JY, Lee JK, Bleazard T, et al. The transcriptional landscape and mutational profile of lung adenocarcinoma. Genome Res 2012;22:2109–19.
29. Williams SV, Hurst CD, Knowles MA. Oncogenic FGFR3 gene fusions in bladder cancer. Hum Mol Genet 2013;22:795–803.
30. Morosini D, Chmielecki J, Goldberg M, Ross JS, Stephens PJ, Miller VA, et al. Comprehensive genomic profiling of sarcomas from 267 adolescents and young adults to reveal a spectrum of targetable genomic alterations. J Clin Oncol 2015;33:suppl; abstr 11020.
31. Davies KD, Mahale S, Astling DP, Aisner DL, Le AT, Hinz TK, et al. Resistance to ROS1 inhibition mediated by EGFR pathway activation in non-small cell lung cancer. PLoS One 2013;8:e82236.
32. Keysar SB, Astling DP, Anderson RT, Vogler BW, Bowles DW, Morton JJ, et al. A patient tumor transplant model of squamous cell cancer identifies PI3K inhibitors as candidate therapeutics in defined molecular bins. Mol Oncol 2013;7:776–90.